Kobe J. Med. Sci., Vol. 52, No. 5, pp. 111-118, 2006

Carotid Artery Occlusion and Collateral Circulation in C57Black/6J Mice Detected by Synchrotron Radiation Microangiography

MASAHIRO TAMAKI[1], KEIJI KIDOGUCHI[1], TAKASHI MIZOBE[1], JUNJI KOYAMA[1], TAKESHI KONDOH[1], TAKASHI SAKURAI[2], EIJI KOHMURA[1], KOICHI YOKONO[2], and KEIJI UMETANI[3]

Departments of [1]Neurosurgery and [2]Geriatric Medicine, Kobe University Graduate School of Medicine

[3]Japan Synchrotron Radiation Research Institute, SPring-8, Sayo-gun, Hyogo, Japan

Received 21 February 2006 /Accepted 15 March 2006

Key words: angiography, carotid artery occlusion, mouse, synchrotron radiation

Using monochromatic synchrotron radiation, we performed microangiography in C57BL/6J mice and investigated their vasculature after unilateral and bilateral carotid artery occlusion. Bilateral occlusion of the carotid artery was made by a ligation of the left common carotid artery followed by a ligation of the right internal carotid artery (ICA) two days later (n=12). Five days after the second surgery, angiography was performed. Unilateral occlusion was made by clipping the right ICA and then angiography was performed immediately (n=5). The control mice did not undergo any occlusion (n=5). We removed the brain of the bilateral occlusion mice after angiography and examined the infarction area. The cerebral microvessels in all animals were clearly visualized. In the control mice, the posterior communicating artery (Pcom) was not visualized. In the unilateral occlusion mice, the anastomosis of the pterygopalatine artery (PPA) and the external carotid artery (ECA) were recognized. The PPA is thus considered to play a role in the collateral vessel between the ICA and the ECA. The Pcom was not visualized. In the bilateral occlusion mice, the Pcom was observed either unilateraly (n=5) or bilateraly (n=5). The Pcom supplied blood flow to the anterior circulation from the vertebrobasilar arteries. The bilateral occlusion mice that had at least one visualized Pcom did not have any infarction. We could successfully visualize the cerebral vasculature of normal mice and carotid artery occluded mice in an in vivo study. Microangiography can demonstrate the development of vasculature and the blood flow dynamics in mice.

Recent advances in molecular technology have enabled us to study the influence of specific genes in cerebral ischemia by using transgenic mice and an increasing number of studies have recently been performed to investigate experimental cerebral ischemia in transgenic mice. The most widely used parent strains for the production of mutants are C57BL/6J and SV129 mice. However, strain-related differences have been reported to exist regarding vulnerability to cerebral ischemia [1-7]. The most likely reason for such strain-related difference is the presence of variations in the cerebrovascular anatomy. The posterior communicating artery (Pcom) is either poorly developed or absent in C57BL/6J. The middle cerebral artery has a larger vascular supplying territory in C57BL/6J than in

Phone: +81-78-382-5966 Fax: +81-78-382-5979 e-mail: tkondo@med.kobe-u.ac.jp

SV129 mice [1]. Such variability in the intracranial vasculature can therefore influence the degree of ischemia [7].

Investigating the cranial vasculature is important for successfully completing mouse ischemic procedures. Beckmann et al. have performed MR high-resolution angiography of the mouse brain [8-10]. They were able to obtain high quality images. They also made vascular resin casts in mice and thus were able to identify small vessels. Cerebral angiography with a contrast agent is an important tool for obtaining serial images on blood flow dynamics in the intracranial vasculature. Conventional angiography could not provide images of the arteries of less than 300 mm in diameter, and it was not sufficient for visualizing small vessels in mice [11]. Recently, both in vivo mice coronary and hepatic angiography using synchrotron radiation have been reported [12-14]. In this study, we investigated the cerebral vasculature of in vivo normal mice and investigated vasculature change after carotid artery occlusion using monochromatic synchrotron radiation using the SPring-8 device (Japan Synchrotron Radiation Research Institute) as the X-ray source, in combination with a high-definition camera and video systems.

MATERIALS AND METHODS

Nine-week-old male C57BL/6J mice (CLEA Japan, Inc.,Tokyo, Japan) were used. All mice were given free access to water and a standard laboratory diet. All procedures were performed under anesthesia with the intraperitoneal injection of pentobarbital (50mg/kg). The rectal temperature was maintained at between 36.5C and 37.5C in all procedures. All animal experiments were conducted according to the guidelines for animal experimentation at Kobe University Graduate School of Medicine.

We used monochromatic synchrotron radiation as an X-ray source. An energy level of 9.0keV was obtained from beamline BL28B2 at the Japan Synchrotron Radiation Research Institute, Hyogo, Japan (SPring-8). The average beam current was 80-100mA. This synchrotron radiation beam energy band was monochromatized and magnified by an asymmetrically cut silicon crystal that was placed in front of the mice. The X-ray flux density at the location of the mice was around $5x10^8$ photons/mm^2/s. The monochromatized X-ray energies just above the iodine K-edge energy was used to produce the highest contrast image of iodine contrast agent. Monochromatic X-rays produced the highest contrast image of iodine contrast medium.

In order to obtain high-resolution real-time images (7 x 9.5 mm, 30 frames / s), a new X-ray SATICON camera (Hitachi Denshi Techno-System, and Hamamatsu Photonics, Japan) was used. The direct-sensing detector consisted of an X-ray direct-sensing pickup tube with a beryllium faceplate for X-ray incidence to the photoconductive layer. The absorbed X-rays in the photoconductive layer were directly converted into photoelectrons and then the signal charges were readout by electron beam scanning. The image signals from the camera were converted into a digital format by an analog-to-digital converter and then were stored in a frame memory with an image format of 755 x 1024 pixels and 10-16 bits/pixels. In a phantom study using a gold bar chart, the limiting spatial resolution measured around 8 μm [15].

The images were stored digitally. The initial acquisition time for an image was 30 images per second. To make the subtraction images, ten original images were added and subtracted by the pre-infusion image.

A PE-50 (427410. Nippon Becton Dickinson Co., I.D.: 0.58mm, O.D.: 0.965mm) was thinned down until reaching a diameter of I.D.: 0.36mm, O.D.: 0.45mm by fire, and then it was used as an injection catheter for the contrast agent. Each mouse was placed in a supine

position under anesthesia. We next incised a 1-cm^2 circle in the right axillary skin. After a sharp dissection, we then inserted the injection catheter into the right subclavian artery. The catheter was secured by a 6-0 nylon ligature (Fig.1.). The trachea was exposed and a tracheal tube was inserted for mechanical ventilation and then angiography was immediately performed.

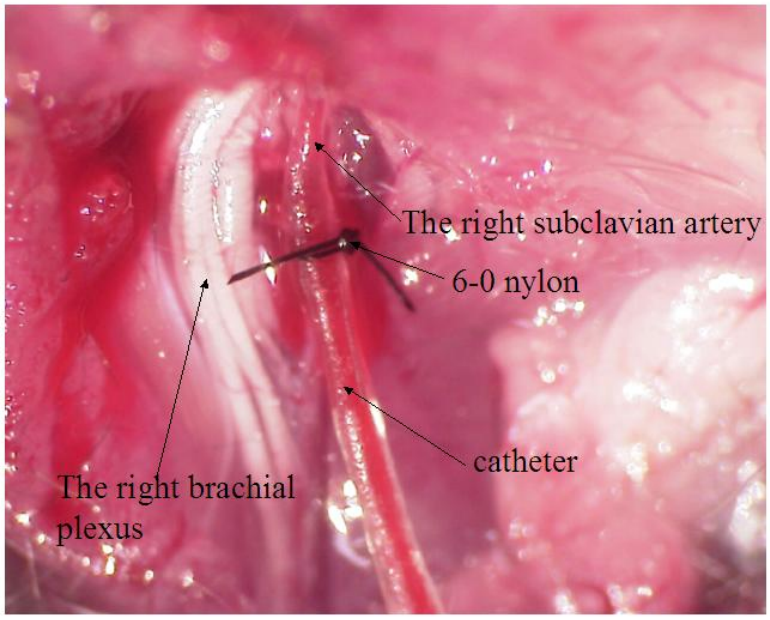

Figure 1. A photograph of catheter insertion in the right subclavian artery.

For chronic bilateral occlusion (n=12), five days prior to angiography, the left CCA was exposed through a midline cervical incision under anesthesia and then it was ligated by 6-0 nylon suture, and cut by microscissors. The wound was thereafter closed with a suture. The second surgery was performed two days after the first surgery. We re-opened the same incision and the right ICA was exposed. The proximal part of the right ICA was coagulated and cut selectively while leaving the ECA intact. The wound was closed. In our pilot study, we found that bilateral CCA ligation resulted in a high mortality probably due to whole brain severe ischemia. An ICA ligation on one side and a CCA ligation on the other side also resulted in a high mortality when the ligations were performed on the same day. Two-stage ligations most likely induce the development of a collateral blood flow, thus leading to less surgical death. After recovering from anesthesia, the mice were allowed free access to food and water. All mice were observed at room temperature for 24h. Three days after the second surgery, cerebral angiography was performed as described above.

For acute unilateral occlusion (n=5), the right ICA was carefully exposed through a midline cervical incision, and a microsurgical clip (Zen temporary clip, Oowa-Tsusho, Tokyo, Japan) was applied to the proximal part of the ICA to acquire the images of immediately after occlusion.

As normal mice (n=5), after catheter insertion and endotracheal intubation, angiography was performed without any occlusion.

Angiography was performed at SPring-8 using the ring experimental hatch of beamline BL28B2. After finishing the procedure, the animals were fixed on an acryl board, and were

injected with pancuronium bromide (2mg/kg) via the injection catheter. Next, under controlled ventilation at 90 / min, we injected 100 ml of half diluted 370 mg I/ml nonionic iodine contrast agent (Iopamiron 370^{R} Nihon Schering, Osaka, Japan) through the catheter with an automated injector for 2 seconds. Serial images were thereafter obtained at 30 pictures / seconds.

Immediately after performing angiography on the bilateral occlusion mice, we decapitated them and then removed their brains carefully. Next, 1-mm thick slices were incubated in normal saline containing 2% 2,3,5-triphenyl tetrazolium chloride (TTC) at room temperature for 30 minutes and then were subsequently stored in 10% phosphate-buffered formalin for observations [16].

RESULTS

The cerebral microvessels were clearly visualized in all mice. In normal mice, we could confirm the right ICA, ECA, pterygopalatune artery (PPA), and vertebrobasilar artery entirely. In addition, a part of contralateral CCA, vertebral artery (VA) were visualized (Fig. 2A). Pcom was not seen in any mice (Fig. 2B). Mean diameter of ICA was 162.6±10.87 μ m.The most minimal diameter of vessels was 30 μ m.

In the unilateral occlusion mice immediately after the right ICA occlusion, the palatine portion of the right PPA was filled retrogradely with the blood flow from the peripheral branch of the right ECA. Next, the right pterygo portion of the PPA and the right ICA were visualized in turn (Fig. 3). These were the early signs of the development of a collateral blood flow from the extracranial blood flow. The Pcom was not seen in those mice.

In bilateral carotid occlusion, the cerebral blood flow is maintained only by the right ECA and the bilateral VAs. The right PPA was filled from the right ECA toward the right ICA, in a manner similar to that of acute unilateral occlusion. In addition, either the unilateral (n=5) or bilateral (n=5) Pcom filled into the ICAs (Fig. 4). In two mice, Pcom was not seen. TTC-staining demonstrated infarction in the left cortex in those two mice, whereas no cerebral infarction was observed in ten bilateral occlusion mice which showed at least one Pcom on angiography (Fig. 5).

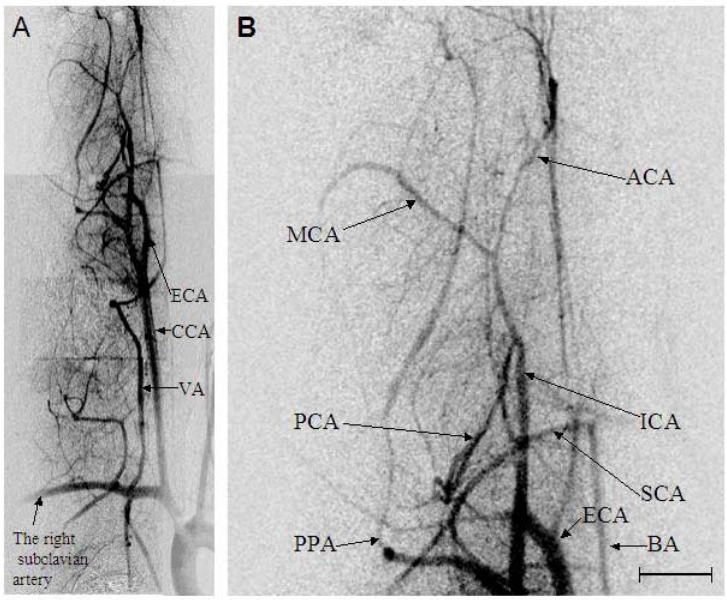

Figure 2. An assembled view **(A)** of brain and neck and an original image with skull **(B)** in normal C57BL/6J mice. Pcom was not visualized. ACA; anterior cerebral artery, BA; basilar artery, CCA; common carotid artery, ECA; external carotid artery, ICA; internal carotid artery, MCA; middle cerebral artery, PCA; posterior cerebral artery, PPA; pterygopalatune artery, SCA; superior cerebellar artery, VA; vertebral artery, bar=1 mm.

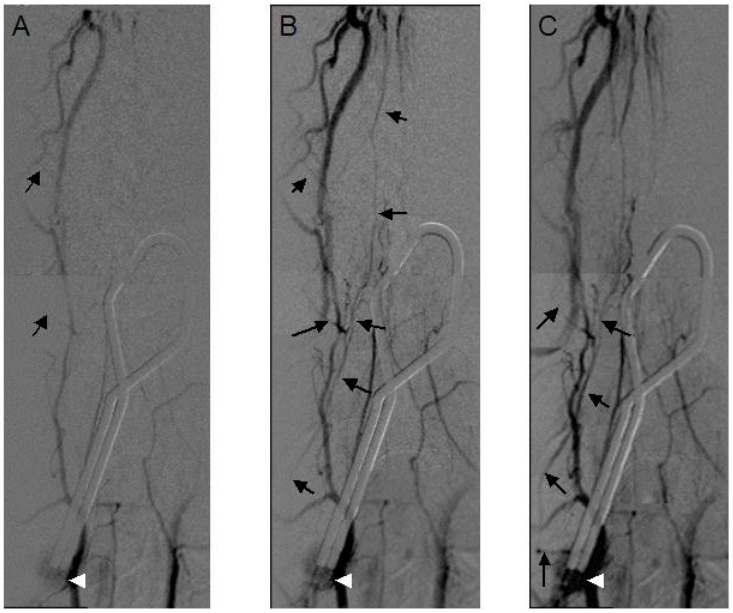

Figure 3. Sequential angiography of unilateral carotid artery occlusion **(A-C).** The right ECA was visualized first at 0.9 seconds **(A)**, then the palatine portion of the right PPA was slowly filled from the peripheral branch of the ECA at 1.2 seconds **(B)** and at 1.5 seconds **(C)**. The black arrows indicate the blood flow in the PPA toward the right ICA. The white arrow head indicates the occluded portion of the ICA.

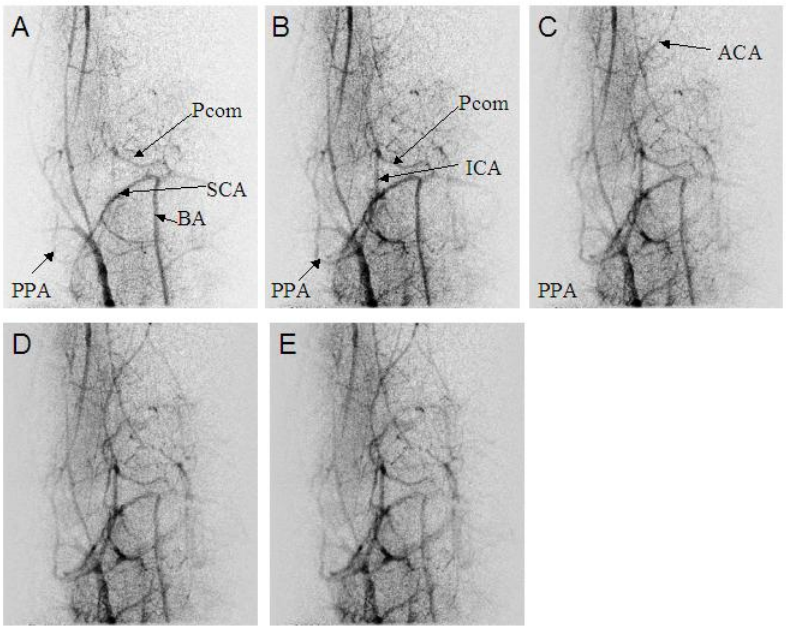

Figure 4. Sequential angiography of bilateral occlusion **(A-E).** The PPA supplied the blood flow into the brain from the ECA though the extracranial portion of the ICA. The right Pcom was visualized. Images were taken at 0.9, 1.2, 1.5, 1.8 and 2.1 seconds from **A** to **E.**

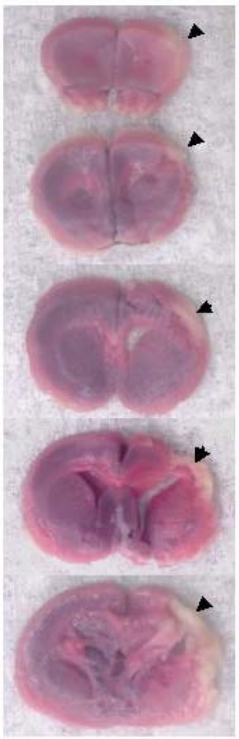

Figure 5. TTC-staining of a bilateral occlusion mouse that did not show Pcom by angiography. Cerebral infarction was observed in the left cerebral cortex (arrow heads).

DISCUSSION

In this in vivo study, we could visualize the cerebral vasculature in normal C57BL/6J mice, while also demonstrating the blood flow direction in carotid occluded mice using monochromatic synchrotron radiation. An injection of contrast agent from the right subclavian artery enabled us to visualize all cranial arteries from their origins, including the aortic arch (Fig. 2). We could thus also clearly observe the venous vasculature (data was not shown).

Beckmann et al. reported MR high-resolution angiograms of the mouse brain [8-10]. The advantages of MR angiography in comparison to our microangiography modality is that MRI can be performed with no contrast agent while also visualizing the images in coronal, sagittal and axial projections. In addition, MRI studies can be done repeatedly on separate days. The drawbacks of MRI are its limitation of spatial resolution which make it impossible to visualize small vessels while it is also unable to show the blood flow direction and dynamics.

With our microangiography method, we have to inject a relatively large quantity of contrast agent to obtain all images from the cervix to the head. We were able to take approximately 10 images in each animal without worsening the background contrast but the use of excessive contrast agent may affect the physiological parameters. Regarding the projection of images, it is possible to obtain other projections such as a sagittal projection by means of changing the position of the platform for mouse, however, the injection of contrast agent is necessary for each projection. The tracheal intubation and administration of muscle relaxant to extinguish any motion artifacts was inevitable to achieve high resolution subtraction images. In other organs in mice, however, microangiography can be performed without tracheal intubation and muscle relaxant [12-14].

The biggest advantage of using an agent is to be able to analyze the blood flow direction and dynamics. In unilateral occlusion, the palatine portion of the right PPA was supplied by the blood flow from the peripheral branch of the right ECA immediately after the right ICA occlusion. The blood flow from the ECA filled into the right ICA in the late phase. We suppose that the anastomosis of the PPA and the ECA existed latently and even immediately after the ICA occlusion the PPA is ready to supply the blood flow to the ICA. In mice, the ophthalmic artery is a branch of the palatine portion of the PPA. In humans, the ophthalmic

artery plays an important role as a collateral vessel between the ECA and the ICA in various types of cerebrovascular disease. In contrast to the PPA, the Pcom was not visualized in either unilateral occlusion or normal mice. Previous reports have shown strain-related differences in the vascular architecture, in particular, the patency of the Pcom, to result in variability in the outcome of cerebral ischemic models [1-7]. A histological study reported that the Pcoms were absent unilaterally in 37.5% or bilaterally in 62.5% of C57BL/6J mice [6]. They exposed the heart, and inserted the catheter into the left ventricle. Thereafter, they infused 5ml of carbon black ink in the condition of cardiac arrest. Our study was performed in more physiological condition. Detection of Pcoms may be affected in experimental condition.

Kitagawa et al. showed the Pcom to be poorly developed in C57BL/6J mice and its diameter was smaller than in other strains [7]. According to our angiography modality, the Pcom was not visualized in normal C57BL/6J mice.

In bilateral occlusion mice, the Pcom was visualized unilaterally (5/12) and bilaterally (5/12) five days after second occlusion and all of these mice survived. In contrast, all ten C57BL/6J mice in our pilot study died within 24 hours when subjected to left ECA occlusion and right ICA occlusion simultaneously. TTC-staining demonstrated infarction in whole ICA territory. This simultaneous occlusion model was fatal. This means that step-wise occlusion which is performed at a 5-day interval is necessary to obtain a sufficient development of the collateral blood flow. The right PPA filled in the right ICA in all those mice. By histology with TTC-staining, we did not find infarcted area in the mice those demonstrated at least one Pcom by angiography. We supposed that the changes of major trunk were due to the dilation of vessels in acute period. Two out of twelve mice with bilateral occlusion had infarction and those two did not demonstrate Pcom by angiography. Whether the mice suffered from cerebral infarction or not depends on the development of the Pcom .

In conclusion, we were able to successfully visualize the cerebral vasculature of in vivo normal mice and carotid artery occluded mice. Microangiography provided us with useful information about the blood flow dynamics. We therefore think it possible to detect the vascular reactivity under drug administration and thereby compare the differences between wild and transgenic mice using microangiography.

ACKNOWLEDGMENTS

This study was supported in part by Grants-in-Aid for Scientific Research, (C)(2)(17591513) to T.K. and (B)(2)(16390410) to E.K. from the Ministry of Education, Science, Sports, and Culture of Japan and by a Grant for Gerontological Research to T.S. from the Novaritis Foundation.

REFERENCES

1. **Maeda, K., Hata, R., Hossmann, K-A.** 1998. Differences in the cerebrovascular anatomy of C57Black/6 and SV129 mice. NeuroReport **9**:1261-1265.
2. **J.C.Wellons, III, Sheng, H., Laskowitz, D.T., Mackensen, G.B., Pearlstein, R.D., Warner, D.S.** 2000. A comparison of strain-related susceptibility in two murine recovery models of global cerebral ischemia. Brain Res **868**:14-21.
3. **Majid, A., He, Y.Y., Gidday, J.M., Kaplan, S.S., Gonzales, ER., Park, T.S., Fenstermacher, J.D., Wei, L., Choi, D.W., Hsu, C.Y.** 2000. Differences in vulnerability to permanent focal cerebral ischemia among 3 common mouse strains. Stroke **31**:2707-2714.

4. **Fujii, M., Hara, H., Meng, W., Vonsattel, J.P., Huang, Z.H., Moskowitz, M.A.** 1997. Strain-related differences in susceptibility to transient forebrain ischemia in SV-129 and C57Black/6 mice. Stroke **28**:1805-1811.
5. **Yang, G., Kitagawa, K., Matsushita, K., Mabuchi, T., Yagita ,Y., Yanagihara, T., Matumoto, M.** 1997. C57BL/6J is most susceptible to cerebral ischemia following bilateral common carotid occlusion among seven mouse strains: selective neuronal death in the murine transient forebrain ischemia. Brain Res **751**:209-218.
6. **Kelly, S., McCulloch, J., Horsburgh, K.** 2001. Minimal ischaemic neuronal damage and HSP70 expression in MF1 strain mice following bilateral common carotid artery occlusion. Brain Res **914**:185-195.
7. **Kitagawa, K., Matsumoto, M., Yang, G., Mabuchi, T., Yagita, Y., Hori, M., Yanagihara,T.** 1998. Cerebral ischemia after bilateral carotid artery occlusion and intraluminal suture occlusion in mice:evaluation of the patency of the posterior communicating artery. J Cereb Blood Flow Metab **18**:570-579.
8. **Beckmann , N., Stirnimann, R., Bochelene, D.** 1999. High resolution magnetic resonance angiography of the mouse brain:application to murine focal cerebral ischemia models. J Magn Reson **140**:442-450.
9. **Beckmann, N.** 2000 High resolution magnetic resonance angiography non-invasively reveals mouse strain differences in the cerebrovascular anatomy in vivo. Magn Reson Med **44**:252-258.
10. **Beckmann, N., Schuler, A., Mueggler, T., Meyer, E.P., Wiederhold, K-H., Staufenbiel, M., Krucker, T.** 2003. Age-Dependent Cerebrovascular Abnormalities and Blood Flow Disturbances in APP23 Mice Modeling Alzheimer's Disease. J Neurosci **17**:8453-8459.
11. **Takahashi, M., Bussaka, H., Nakagawa, N.** 1984.Evaluation of the cerebral vasculature by intraarterial DSA-with emphasis on in vivo resolution. Neuroradiology **26**:253-259.
12. **Yamashita, T., Kawashima, S., Ozaki, M., Namiki, M., Hirase, T., Inoue, N., Hirata, K., Umetani, K., Sugimura, K., Yokoyama, M.** 2002. Mouse coronary angiography using synchrotron radiation microangiography. Circulation **105**:e3-e4.
13. **Yamashita, T., Kawashima, S., Ozaki, M., Namiki, M., Shinohara, M., Inoue, N., Hirata, K., Umetani, K., Yokoyama, M.** 2002. In vivo angiographic detection of vascular lesions in apolipoprotein E-knockout mice using a synchrotron radiation microangiography system. Circ J **66**:1057-1059.
14. **Kobayashi, S., Hori, M., Dono, K., Nagano, H., Umeshita, K., Nakamori, S., Sakon, M., Osuga, K., Umetani, K., Murakami, T., Nakamura, H., Monden, M.** 2004. In vivo real-time microangiogaphy of the liver in mice using synchrotron radiation. J Hepatol **40**:405-408.
15. **Umetani, K., Itasaka, S., Ogura, M., Kimura, H., Hiraoka, M.** 2001. Synchrotron radiation microangiography system for observation of blood flow in murine tumor vasculature. Bioimage **9**:97-106.
16. **Goldlust, E.J., Paczynski, R.P., He, Y.Y., Hsu, C.Y., Goldberg, M.P.** 1996. Automated measurement of infarct size with scanned images of triphenyltetrazolium chloride-stained rat brain. Stroke **27**:1657-1662.